1-Hydroxy-xanthine derivatives inhibit the human Caf1 nuclease and Caf1-containing nuclease complexes via Mg^{2+}-dependent binding

Blessing Airhihen[1,#], Lorenzo Pavanello[1,†], Gopal P. Jadhav[2,‡], Peter M. Fischer[2] and Gerlof Sebastiaan Winkler[1]

1 School of Pharmacy, University of Nottingham, UK
2 School of Pharmacy, Centre for Biomolecular Sciences, University of Nottingham, UK

Correspondence

G. S. Winkler, School of Pharmacy, University of Nottingham, East Drive, University Park, Nottingham NG7 2RD, UK
Tel: +44 (0) 115 8468457
E-mail:sebastiaan.winkler@nottingham.ac.uk

#Permanent address

Department of Pharmacology, School of Pharmacy, Niger Delta University, Wilberforce Island, Nigeria

†Present address

Domainex Ltd, Chesterford Research Park, Little Chesterford, Saffron Walden, Essex, UK

‡Present address

School of Medicine, Department of Clinical & Translational Sciences, Creighton University, Omaha, NE, USA

In eukaryotic cells, cytoplasmic mRNA is characterised by a 3′ poly(A) tail. The shortening and removal of poly(A) tails (deadenylation) by the Ccr4-Not nuclease complex leads to reduced translational efficiency and RNA degradation. Using recombinant human Caf1 (CNOT7) enzyme as a screening tool, we recently described the discovery and synthesis of a series of substituted 1-hydroxy-3,7-dihydro-1*H*-purine-2,6-diones (1-hydroxy-xanthines) as inhibitors of the Caf1 catalytic subunit of the Ccr4-Not complex. Here, we used a chemiluminescence-based AMP detection assay to show that active 1-hydroxy-xanthines inhibit both isolated Caf1 enzyme and human Caf1-containing complexes that also contain the second nuclease subunit Ccr4 (CNOT6L) to a similar extent, indicating that the active site of the Caf1 nuclease subunit does not undergo substantial conformational change when bound to other Ccr4-Not subunits. Using differential scanning fluorimetry, we also show that binding of active 1-hydroxy-xanthines requires the presence of Mg^{2+} ions, which are present in the active site of Caf1.

In eukaryotes, cytoplasmic mRNA is characterised by the presence of a 3′ poly(A) tail. Poly(A) tail length is broadly distributed with the median length varying from 27–28 nucleotides in yeast to 40–100 nucleotides in mammalian cells [1,2]. The poly(A) tail contributes to mRNA stability and translational efficiency, and

the removal of the poly(A) tail is an important step in regulated mRNA degradation [3,4]. A key multi-subunit enzyme complex involved in the controlled removal of the poly(A) tail is the Ccr4-Not deadenylase complex that is composed of two catalytic nuclease subunits and six noncatalytic components. In mammalian cells, the large subunit CNOT1 is the scaffold of the complex [5,6]. Its N-terminal domain interacts with CNOT11 and CNOT10, whose function is not well understood [6,7]. The MIF4G domain of CNOT1 is part of the nuclease module and binds to the Caf1 catalytic subunit (encoded by either *CNOT7* or *CNOT8*), which in turn interacts with the leucine-rich repeat domain of the second catalytic subunit Ccr4 (encoded by *CNOT6* or *CNOT6L*) [8,9]. The DUF3819 domain of CNOT1 binds to CNOT9 [10,11], while the C-terminal region of CNOT1 interacts with the CNOT2 and CNOT3 subunits forming the NOT-module [12,13]. The noncatalytic subunits stimulate the activity of the nuclease module [14,15] and form a platform for interactions with regulators of mRNA stability, including the GW182/TNRC6 component of the microRNA repression complex [16,17], and the AU-rich element binding protein tris-tetraprolin TTP (ZFP36) [18–20]. Using genetically modified mice, specific physiological roles for a number of Ccr4-Not components have been uncovered. The Caf1 nuclease subunit encoded by the *Cnot7* gene regulates bone formation by inhibiting osteoblast activity [21] and is also required for male fertility [22,23]. Deletion of one copy of *Cnot3*, a noncatalytic subunit of Ccr4-Not, protects against obesity in mice [24]. Mutations in Ccr4-Not components have also been implicated in human disease. Nonsense mutations in *CNOT3* are associated with acute lymphoblastic leukaemia, whereas a recurrent missense mutation in *CNOT9* is found in metastatic melanoma [25,26]. Furthermore, mouse models of breast cancer have implicated Ccr4-Not components in promoting metastatic cancer [27,28]. In case of Caf1, its enzymatic activity is required for this effect indicating that Caf1 inhibitors may be useful pharmacological tools to validate this protein as a possible drug target to prevent metastatic breast cancer [28].

Although much progress has been made in the past few years, the mechanism of poly(A) deadenylation by Caf1 and Ccr4 is still not fully understood. The Caf1 subunit, which contains an RNAse D/DEDD (Asp-Glu-Asp-Asp) nuclease domain, appears dispensable in budding yeast, but makes a contribution to the activity of the complex in fission yeast and the fruit fly [29–31]. On the other hand, the second catalytic nuclease subunit, the EEP (endonuclease–exonuclease–phosphatase) domain protein Ccr4, is the catalytic subunit in budding yeast and – like Caf1 – contributes to the activity in fission yeast and *Drosophila* [15,32–34]. The situation is more complex in human cells, where both Caf1 and Ccr4 appear to be required for activity of the nuclease module, which has much increased activity as compared to either the isolated Caf1 or Ccr4 subunit [35]. Moreover, it has been proposed that the Caf1 and Ccr4 subunits have specialised roles, with Ccr4 required for the degradation of poly(A) bound by the poly(A)-binding protein PABPC1, which inhibits the activity of Caf1 [36,37]. On the other hand, it has been reported that the highly similar proteins BTG1 and BTG2 can mediate interactions between PABPC1 and Caf1, thereby promoting deadenylation by Caf1 [38].

Recently, we reported the discovery and synthesis of a series of substituted 1-hydroxy-3,7-dihydro-1*H*-purine-2,6-dione (1-hydroxy-xanthine) compounds as the first non-nucleoside inhibitors of Caf1 [39]. Here, we report the further biochemical characterisation of these compounds by using two assays: (a) a chemiluminescence-based assay for the detection of AMP, the product of the deadenylation reaction; and (b) differential scanning fluorimetry (thermal shift assay). Using these assays, we demonstrate that the 1-hydroxy-xanthine compounds inhibit the isolated human Caf1 enzyme with the same potency as human Caf1-containing complexes that also contain the second catalytic subunit Ccr4. This suggests that the active site of Caf1 does not undergo substantial conformational changes when incorporated into the Ccr4-Not complex. In addition, we show that active 1-hydroxy-xanthines require the presence of Mg^{2+} ions for binding, which provides experimental support for the proposed role of the *N*-hydroxyimide moiety
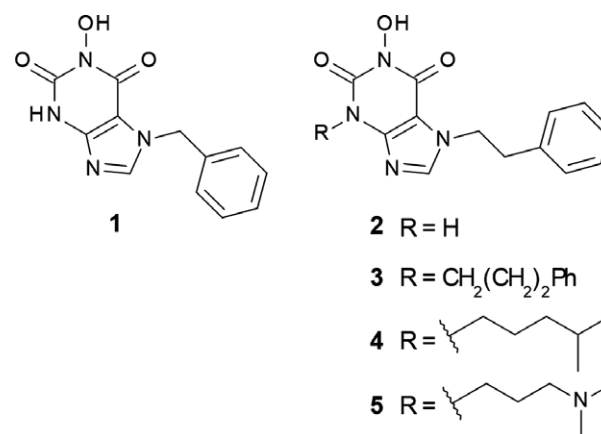

Fig. 1. Structure of 1-hydroxy-xanthine derivatives **1–5**.

in coordinating Mg^{2+} ions present in the active site of Caf1. These experiments also demonstrate the value of the chemiluminescence-based AMP detection assay and differential scanning fluorimetry as useful orthogonal assays that supplement our previously reported fluorescence-based FRET assay [40] for the discovery and characterisation of inhibitors of the Caf1 nuclease enzyme.

Materials and methods

Reagents

1-Hydroxy-xanthine compounds **1**–**5** were described previously [39]. The human Caf1/CNOT7 enzyme was expressed and purified from *Escherichia coli* BL21 (DE3) using procedures described before [40]. The trimeric human nuclease
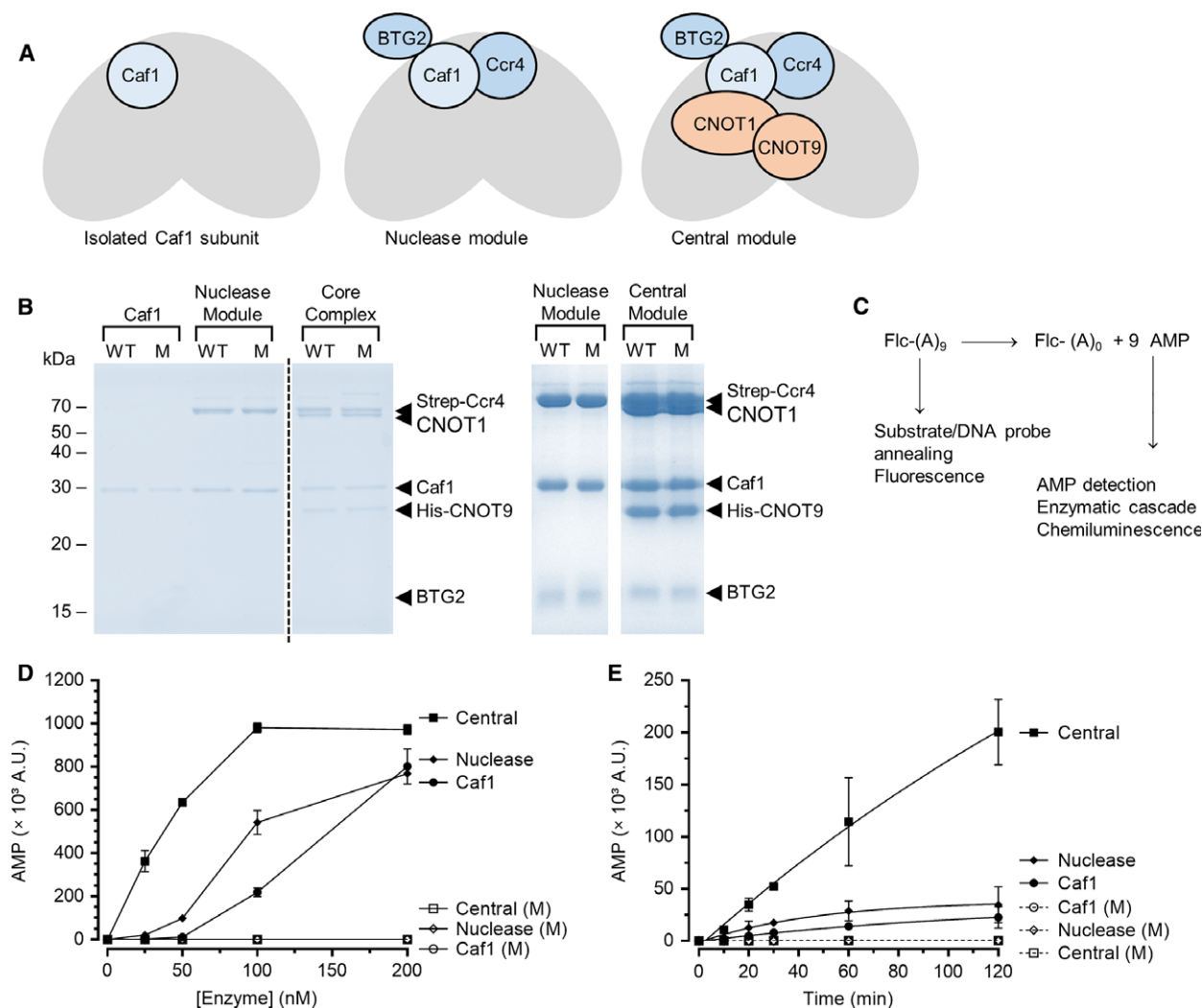

Fig. 2. Application of a chemiluminescence-based AMP detection system as a quantitative assay for deadenylation activity. (A) Schematic overview of Caf1 and Caf1-containing complexes. (B) Purified recombinant Caf1 and Caf1-containing complexes. WT, wild-type; M, mutant protein preparations containing the D40A amino acid substitution in Caf1 or the D40A substitution in Caf1 and the E240A substitution in Ccr4 (nuclease and central modules). *Left panel*, purified proteins (5 μg) were separated by 14% SDS/PAGE and stained with Coomassie Brilliant Blue. *Right panel*, purified proteins (20 μg) were separated by 14% SDS/PAGE and stained with Coomassie Brilliant Blue. (C) Schematic of the deadenylation reaction and the use of activity assays based on RNA substrate (*left*) and AMP product (*right*) detection. The fluorescence-based assay was described before [40]. (D) Activity of Caf1 and Caf1-containing complexes using chemiluminescence-based AMP detection. Protein samples were incubated with a synthetic RNA substrate at 30 °C for 60 min before the detection of AMP levels. (E) Time-course analysis of Caf1 and Caf1-containing complexes. Protein samples (25 nM) were incubated with a synthetic RNA substrate containing 9 terminal adenosine residues (1.0 μM) at 30 °C. A.U., arbitrary units. Error bars represent the standard error of the mean (*n* = 3).

module (BTG2-Caf1/CNOT7-Ccr4/CNOT6L) was obtained by co-expression of the three proteins using plasmids pQE80L-BTG2 and pACYC-Duet1-Strep-CNOT6L-CNOT7 and purified as described before [14,35]. The human pentameric central module (BTG2-Caf1/CNOT7-Ccr4/CNOT6L-CNOT1-CNOT9) of Ccr4-Not was obtained by reconstitution of the complex after separate expression and purification of the nuclease module and the dimeric complex composed of CNOT1 (MIF4G and DUF3819 domains; amino acids 1093–1595) and CNOT9 (ARM domain; amino acids 33–283) using plasmid pACYC-Duet1-CNOT1-CNOT9 as described before [14].

Enzyme activity assays

Standard reaction conditions for deadenylase assays (10 μL) were as follows: 25 nM enzyme, 20 mM Tris/HCl pH 7.9, 50 mM NaCl, 2 mM $MgCl_2$, 10% glycerol, 1 mM β-mercaptoethanol and 1.0 μM 5′-Flc-labelled RNA substrate in nuclease-free water as described before [40]. Reactions containing inhibitory compounds also contained 5% DMSO. After incubation at 30 °C for 60 min, chemiluminescence-based detection of AMP was carried out using the AMP-Glo kit (Promega, Southampton, Hampshire, UK) [41–43]. To this end, 5 μL of the enzyme reaction was mixed with an equal volume of AMP-Glo reagent I in a white 96-well half-area multiwell plate (Corning Costar, reference 3693). After a further 60-min incubation at room temperature, 10 μL AMP-Glo reagent II was added. After another 60-min incubation at room temperature, chemiluminescence was measured using a GloMax 96 multiwell plate luminometer (Promega). Data were exported to Microsoft Excel 2013 and analysed using GRAPHPAD PRISM (version 7).

Differential scanning fluorimetry

Differential scanning fluorimetry (thermal stability assay) was carried out as described with minor modifications using an Agilent MX3005p instrument and the fluorescent dye SYPRO Orange (5000 × in DMSO, Thermo Fisher Scientific, Loughborough, Leicestershire, UK) [44]. Standard assays (20 μL) contained the following: 2 μM purified Caf1/CNOT7 enzyme, 20 mM Tris/HCl pH 7.8, 50 mM NaCl, 10% glycerol, 1 mM β-mercaptoethanol, 0.2 × SYPRO Orange dye, 100 μM compound, 5% DMSO. Assays carried out in the presence of divalent metal ions also contained 2 mM $MgCl_2$.

Reactions were performed in thin-wall, PCR grade 96-well plates with V-shaped wells. After sealing using optically clear lids, reactions were thoroughly mixed and collected at the bottom of the wells by centrifugation. Fluorescence scanning was carried out using a temperature gradient from 25 °C to 95 °C at 1 °C per minute using the FAM (492 nm) filter for excitation and the ROX (610 nm) filter for detection. Each experiment contained three technical replicates. Data were acquired using MXPRO QPCR software (Agilent, Stockport, Cheshire, UK), exported to Microsoft Excel 2013, and analysed using publicly available macros for Microsoft Excel 2013 and templates for GRAPHPAD PRISM (version 7) as described [44].

Statistical analysis

Standard errors of the mean were calculated using GRAPHPAD PRISM (version 7). Reported IC_{50} values were determined based on at least three independent experiments each containing at least two technical replicates. Reported ΔT_m values were calculated based on at least three

Table 1. Activity of 3,7-disubstituted-1-hydroxy-1,7-dihydro-1*H*-purine-2,6-diones.

Cmpd	IC_{50} (μM) *vs* Caf1 (Reference)[a]	IC_{50} (μM) *vs* Caf1[b]	IC_{50} (μM) *vs* trimeric Caf1-complex[c]	IC_{50} (μM) *vs* pentameric Caf1-complex[d]	Differential scanning fluorimetry	
					ΔT_m (°C) Caf1 (no $MgCl_2$)[e]	ΔT_m (°C) Caf1 ($MgCl_2$)[f]
1	10.4 ± 0.4	12.7 ± 0.9	13.6 ± 0.6	10.8 ± 0.2	−0.4 ± 0.3	2.4 ± 0.3
2	1.5 ± 0.3	3.2 ± 0.4	2.3 ± 0.2	2.6 ± 0.3	0.6 ± 0.4	4.1 ± 0.3
3	2.1 ± 0.3	2.7 ± 0.3	2.4 ± 0.2	2.4 ± 0.1	0.5 ± 0.5	3.3 ± 0.2
4	1.7 ± 0.4	2.2 ± 0.3	2.2 ± 0.1	2.5 ± 0.4	0.6 ± 0.6	3.4 ± 0.4
5	0.59 ± 0.11	0.79 ± 0.09	1.0 ± 0.2	0.98 ± 0.07	−0.2 ± 0.3	4.7 ± 0.3

[a]IC_{50} values determined using a fluorescence-based assay were taken from Jadhav *et al.* [39].
[b]IC_{50} values were determined using chemiluminescence-based AMP detection in the presence of monomeric Caf1/CNOT7 enzyme.
[c]IC_{50} values were determined using chemiluminescence-based AMP detection in the presence of trimeric BTG2-Caf1-Ccr4 nuclease module.
[d]IC_{50} values were determined using chemiluminescence-based AMP detection in the presence of pentameric BTG2-Caf1-Ccr4-CNOT1-CNOT9 central module.
[e]Differential scanning fluorimetry. ΔT_m values were determined by differential scanning fluorimetry in the presence of Caf1/CNOT7 and the indicated compound.
[f]Differential scanning fluorimetry. ΔT_m values were determined by differential scanning fluorimetry in the presence of Caf1/CNOT7, 2 mM $MgCl_2$ and the indicated compound. Indicated are the mean ± standard error of the mean ($n = 3$).

independent experiments, each containing three technical replicates. *P* values were calculated using a two-tailed *t*-test (GRAPHPAD PRISM, version 7).

Results and Discussion

Chemiluminescence-based detection of AMP as a sensitive assay for deadenylase activity

To determine the activity of 1-hydroxy-xanthine compounds (Fig. 1) versus human Caf1 and Caf1-containing complexes that also contain the second catalytic subunit Ccr4, we first purified the isolated Caf1 protein, which displays relatively weak deadenylase activity, the trimeric BTG2-Caf1-Ccr4 nuclease module, which displays relatively robust nuclease activity, and the pentameric central module, which displays relatively high enzymatic activity (Fig. 2A). The proteins were expressed in *Escherichia coli* and were purified using affinity chromatography as described before (Fig. 2B) [14,35,40]. We then evaluated the use of chemiluminescence-based detection of AMP [41–43] as an activity assay of Caf1 and Caf1-containing complexes. We chose this assay as a potential assay that is complementary to the fluorescence-based assay described before (Fig. 2C) [40]. Importantly, the AMP detection assay is suitable for multiwell plates, allowing the analysis of many compounds in parallel, and does not depend on time-consuming analysis of reaction products by gel electrophoresis.

We used a synthetic 15-mer RNA oligonucleotide with nine adenosines at the 3′ end as the enzyme substrate [40]. After incubation with varying concentrations of the Caf1 enzyme, AMP was detected in a two-step procedure. In the first step, AMP was enzymatically converted to ADP. Then, enzymatic conversion of ADP to ATP in the presence of luciferase and luciferin resulted in chemiluminescence proportional to the amount of AMP produced in the reaction. Robust levels of AMP were detected at enzyme concentrations below 100 nM, which is substantially lower as compared to the amount of enzyme required for the fluorescence-based assay (Fig. 2D,E) [40]. Only very low levels of AMP were produced in the presence of the catalytically inactive variant D40A, and a signal/background ratio > 10 was achieved at wild-type enzyme concentrations > 25 nM (Fig. 2D,E). When the activity of Caf1-containing complexes was determined, much increased levels of AMP were detected in agreement with our previous findings that the activity of the nuclease and central modules of Ccr4-Not display higher activity than the isolated Caf1 subunit [14,35]. The activity determined in the
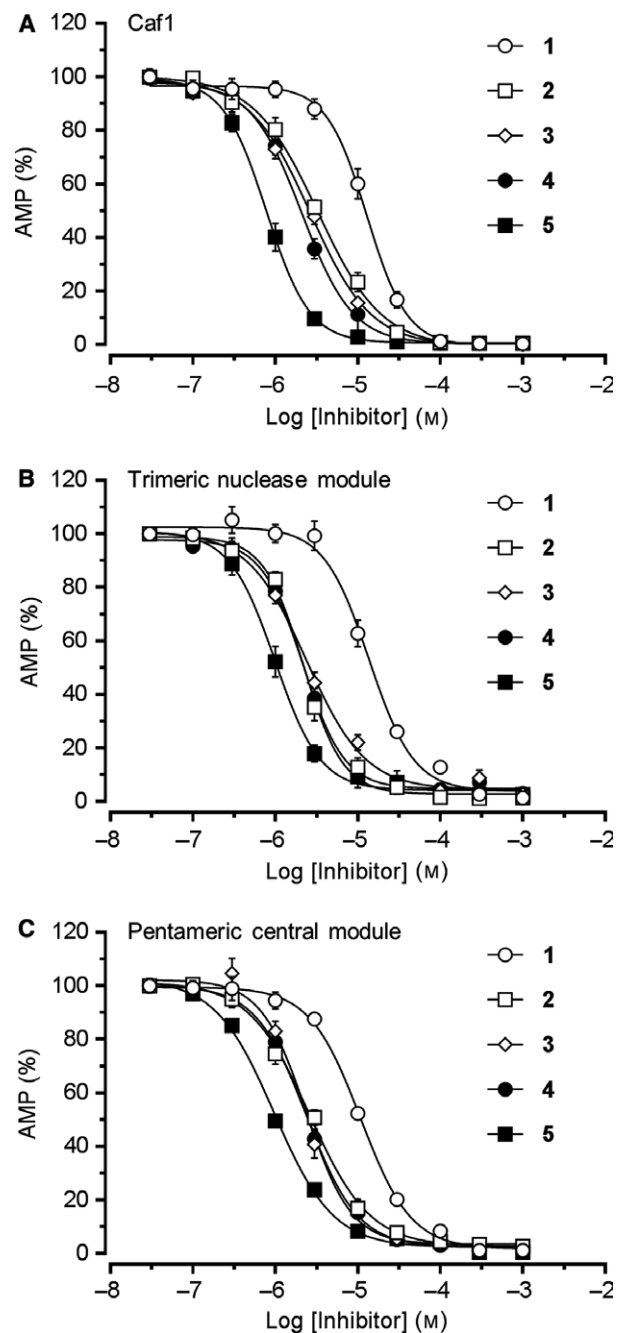

Fig. 3. Inhibition of Caf1 and Caf1-containing complexes by 1-hydroxy-xanthines. (A) Inhibition of the isolated Caf1 subunit. (B) Inhibition of a trimeric BTG2-Caf1-Ccr4 nuclease module of Ccr4-Not. (C) Inhibition of a pentameric BTG2-Caf1-Ccr4-CNOT1-CNOT9 central module of Ccr4-Not. Enzyme preparations (25 nM) were incubated with a synthetic RNA substrate containing nine terminal adenosine residues (1.0 μM) at 30 °C for 60 min. Error bars represent the standard error of the mean (*n* = 3).

presence of Caf1-containing complexes was specific, because only very low levels of AMP were detected in the presence of Caf1-containing complexes with

inactive Caf1 (D40A) and Ccr4 (E240A) catalytic subunits.

Together, these experiments demonstrate that chemiluminescence-based detection of AMP is a highly sensitive assay that is suitable for the evaluation of the enzymatic activity of Caf1 and Caf1-containing complexes.

1-Hydroxy-xanthine compounds inhibit Caf1 and Caf1-containing complexes with similar potency

To test whether the assay can be used as a quantitative assay for the characterisation of small-molecule inhibitors, we next determined the IC_{50} value of five 1-hydroxy-xanthine compounds **1**–**5**, which were previously characterised using the fluorescence-based assay and inhibit Caf1 with IC_{50} values ranging from 0.59 ± 0.11 μM to 10.4 ± 0.4 μM (Fig. 1 and Table 1) [39]. Importantly, these compounds do not display activity towards the catalytic domain of Ccr4 [39]. To determine the IC_{50} values, we used conditions where the reaction product increased proportionally with time and substrate concentrations were not limiting (Fig. 2E, $t = 60$ min). As shown in Fig. 3A and Table 1, the IC_{50} values determined using chemiluminescence-based AMP detection closely matched the values previously obtained using the fluorescence-based assay. Based on these results, we conclude that both assays are suitable for the characterisation of the activity of compounds that inhibit deadenylase enzymes and result in comparable IC_{50} values.

To determine whether our recently developed series of 1-hydroxy-xanthines inhibit Caf1-containing complexes with similar potency compared to the isolated

Caf1 subunit, we next determined the activity of compounds **1**–**5** versus the trimeric nuclease module and the pentameric central module of the Ccr4-Not complex (Fig. 3B,C). As shown in Fig. 3 and Table 1, the selected 1-hydroxy-xanthines displayed similar activity versus the trimeric nuclease module (Fig. 3B) as well as the pentameric central module (Fig. 3C). These results indicate that the active site of the isolated Caf1 subunit does not undergo substantial conformational changes upon association with other Ccr4-Not subunits, including the Ccr4 ribonuclease subunit, whose leucine-rich repeat (LRR) domain interacts directly with the Caf1/CNOT7 subunit, or the CNOT1 subunit, which binds to Caf1 via the MIF4G domain. Moreover, the compounds fully inhibited the activity of Caf1 and the Caf1-containing nuclease complexes showing that the Caf1 subunit is indispensable for deadenylase activity in the context of the nuclease and central modules, even in the presence of the second catalytic nuclease subunit Ccr4.

1-Hydroxy-xanthine compounds require the presence of Mg^{2+} ions for binding

Having established that 1-hydroxy-xanthines inhibit Caf1 and Caf1-containing complexes with similar potency, we next aimed to obtain further information about their mode of binding. Specifically, we aimed to establish if binding of 1-hydroxy-xanthines requires the presence of Mg^{2+} ions in the active site as suggested by our proposed binding mode [39] or that of related compounds containing an *N*-hydroxyimide moiety to the influenza endonuclease PA protein and the human DNA structure-specific endonuclease FEN-
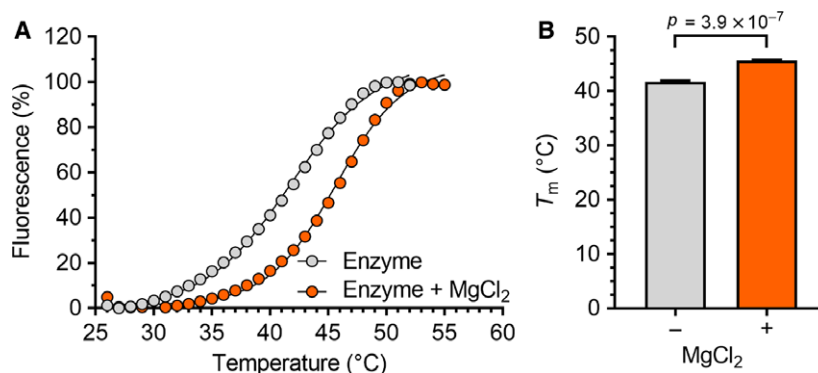

Fig. 4. Increased thermal stability of Caf1 in the presence of Mg^{2+} ions. (A) Differential scanning fluorimetry of Caf1 in the absence and presence of $MgCl_2$. Caf1 (2 μM) was incubated in the absence or presence of 2 mM $MgCl_2$ and the SYPRO Orange dye. Fluorescence scanning was carried out using a temperature gradient from 25 °C to 95 °C. The melting temperature T_m was determined as described [44]. (B) Thermal stability of Caf1 in the absence and presence of $MgCl_2$. $\Delta T_m = 3.9 \pm 0.2$ °C; mean $\pm$ SEM ($n = 7$). Error bars indicate the standard error of the mean ($n = 7$).

1 [45–48]. To this end, we evaluated the use of differential scanning fluorimetry (DSF), which is based on increased thermal stability of a protein induced upon binding of small-molecule ligands [44,49,50]. First, we determined the melting temperature T_m of Caf1 in the absence and presence of $MgCl_2$ and observed a robust increase in the T_m of Caf1 in the presence of Mg^{2+} ions (Fig. 4; $\Delta T_m = 3.9 \pm 0.2$ °C; mean $\pm$ SEM,
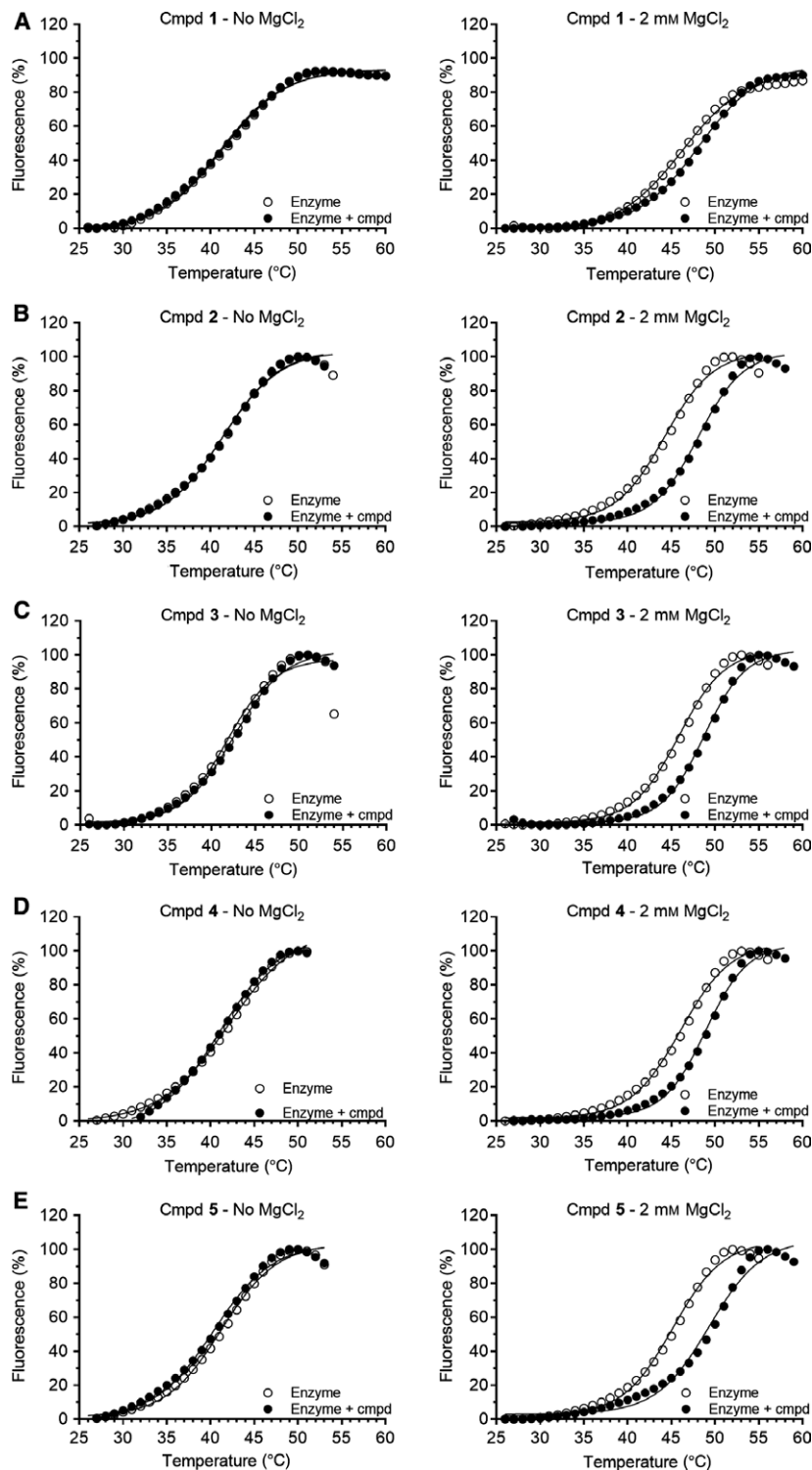

Fig. 5. Binding of 1-hydroxy-xanthines requires the presence of Mg^{2+} ions. (A-E) Representative experiments showing binding of compounds **1**–**5** to Caf1 in the absence of Mg^{2+} (*left panels*) and 2 mM $MgCl_2$ (*right panels*). Compounds (100 μM) were incubated with Caf1 (2 μM) and the SYPRO Orange dye. Fluorescence scanning was carried out using a temperature gradient from 25 °C to 95 °C. The melting temperature T_m was determined as described [44].

$n = 7$). Encouraged by these results, we then carried out DSF using Caf1 in the presence of 1-hydroxy-xanthines **1**–**5**. In the absence of $MgCl_2$, no significant changes in the melting temperatures were observed in the presence of compounds **1**–**5** as compared to enzyme only ($P > 0.05$; Table 1 and Fig. 5). By contrast, significant changes in the thermal shifts were observed in the presence of compound **1**–**5** and $MgCl_2$ as compared to control reactions containing enzyme and $MgCl_2$ only ($P < 0.05$). These observations suggest that binding of 1-hydroxy-xanthines requires the presence of Mg^{2+} ions, which are present in the active site of Caf1.

Correlation between thermal shifts and IC_{50} values

Because it has been shown that thermal shift assays can provide quantitative information about the binding affinity of enzyme ligands [50], we next considered whether the observed thermal shifts correlated with the IC_{50} inhibitory concentrations of compounds **1**–**5**. To this end, we plotted the ΔT_m values observed in the presence of $MgCl_2$ against the corresponding IC_{50} values. As shown in Fig. 6, we found a high correlation between the ΔT_m values and the pIC_{50} values obtained using the isolated Caf1 enzyme ($r^2 = 0.90$ using the fluorescence-based FRET assay and $r^2 = 0.78$ using the chemiluminescence-based AMP detection assay). This indicates that the observed thermal shifts provide quantitative information about the relative potency of compounds **1**–**5** (Fig. 6) versus the Caf1 nuclease. Thus, we show that differential scanning fluorimetry is not only useful to provide information about the binding mode of Caf1 inhibitors, but may also be used as an additional screening tool to characterise and identify new compounds that inhibit the Caf1 nuclease.

In summary, the results reported here provide insight into the mechanism of inhibition of the Caf1 deadenylase enzyme by 1-hydroxy-xanthines. First, we show that compounds **1**–**5** inhibit the isolated enzyme with similar potency as Caf1-containing complexes, which also include the Ccr4 nuclease subunit. It is notable that the activity of the Caf1-containing complexes was completely inhibited at higher compound concentrations, even though the compounds do not affect Ccr4 [39]. This indicates that Caf1 is essential for the activity of complexes containing both Caf1 and Ccr4 nucleases. The observation that the nuclease complexes can be inhibited by small molecules extends our previously reported findings, which showed that the activity of the human BTG2-Caf1-Ccr4 nuclease complex requires the activity of both Caf1 and Ccr4, and that inactivating amino acid substitutions in either Caf1 or Ccr4 are sufficient to abolish the activity of the complex [35]. This contrasts with the finding that Caf1 activity is not essential for the activity of complexes containing the Caf1 and Ccr4 nucleases from the fission yeast *S. pombe* and the fruit fly *Drosophila* and residual activity is observed upon inactivation of Caf1 in those cases [15,33]. Secondly, we showed that binding of compounds **1**–**5** requires the presence of Mg^{2+} ions, which bind in the active site of Caf1. This is in agreement with the proposed role of the *N*-hydroxyimide moiety in 1-hydroxy-xanthines and related compounds forming ion–dipole interactions with the Mg^{2+} ions [45–48].

In addition to these findings, two further assays for the evaluation of Caf1 inhibitors are presented here. The chemiluminescence-based detection of AMP provides an orthogonal assay for our previously reported fluorescence-based assay that does not depend on gel-based product analysis. While the AMP detection method has some disadvantages, including the relative instability of the signal and the dependence on an
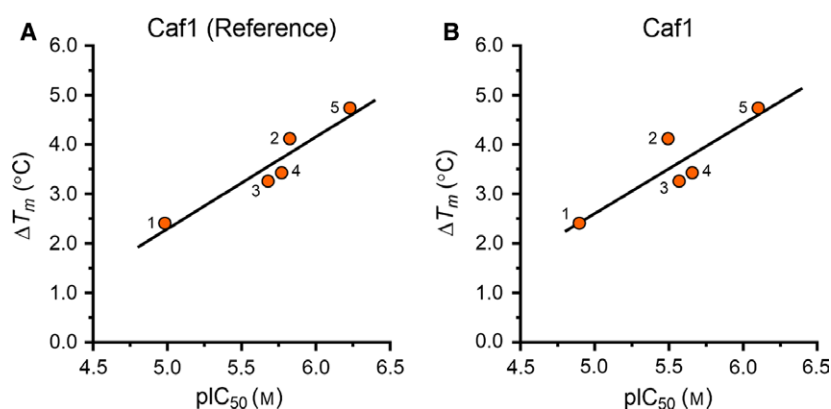

Fig. 6. Correlation between thermal shifts (ΔT_m) observed in the presence of $MgCl_2$ and inhibitory activity of compounds **1**–**5**. (A) Correlation between thermal shift and pIC_{50} values determined using the isolated Caf1 protein and the fluorescence-based assay ($r^2 = 0.90$). (B) Correlation between thermal shift and pIC_{50} values determined using the isolated Caf1 protein and the chemiluminescence-based AMP detection assay ($r^2 = 0.78$). Linear regression was carried out using GRAPHPAD PRISM (version 7.0).

enzymatic cascade for detection of AMP, which requires additional time-consuming incubation steps, it benefits from increased sensitivity, a greater dynamic range and increased signal-to-noise ratios. In addition, we show that the widely used thermal shift assay is suitable for the analysis of inhibitor binding to Caf1 and also provides information about the binding mode of the inhibitor–enzyme complexes.

Acknowledgements

Author contributions

GSW conceived the experiments. BA, LP and GSW designed the experiments. BA and LP carried out the experiments. GPJ and PMF contributed unique reagents. BA, LP and GSW analysed the data. BA, LP, PMF and GSW contributed to the preparation of the manuscript.

Conflict of interest

The authors declare no conflict of interest.

References

1 Chang H, Lim J, Ha M and Kim VN (2014) TAIL-seq: Genome-wide determination of poly(A) tail length and 3′ end modifications. *Mol Cell* **53**, 1044–1052.

2 Subtelny AO, Eichhorn SW, Chen GR, Sive H and Bartel DP (2014) Poly(A)-tail profiling reveals an embryonic switch in translational control. *Nature* **508**, 66–71.

3 Jonas S and Izaurralde E (2015) Towards a molecular understanding of microRNA-mediated gene silencing. *Nat Rev Genet* **16**, 421–433.

4 Wahle E and Winkler GS (2013) RNA decay machines: deadenylation by the Ccr4-Not and Pan2-Pan3 complexes. *Biochim Biophys Acta* **1829**, 561–570.

5 Bai Y, Salvadore C, Chiang YC, Collart MA, Liu HY and Denis CL (1999) The CCR4 and CAF1 proteins of the CCR4-NOT complex are physically and functionally separated from NOT2, NOT4, and NOT5. *Mol Cell Biol* **19**, 6642–6651.

6 Bawankar P, Loh B, Wohlbold L, Schmidt S and Izaurralde E (2013) NOT10 and C2orf29/NOT11 form a conserved module of the CCR4-NOT complex that docks onto the NOT1N-terminal domain. *RNA Biol* **10**, 228–244.

7 Mauxion F, Preve B and Seraphin B (2013) C2ORF29/CNOT11 and CNOT10 form a new module of the CCR4-NOT complex. *RNA Biol* **10**, 267–276.

8 Basquin J, Roudko VV, Rode M, Basquin C, Seraphin B and Conti E (2012) Architecture of the nuclease module of the yeast Ccr4-not complex: the Not1-Caf1-Ccr4 interaction. *Mol Cell* **48**, 207–218.

9 Petit AP, Wohlbold L, Bawankar P, Huntzinger E, Schmidt S, Izaurralde E and Weichenrieder O (2012) The structural basis for the interaction between the CAF1 nuclease and the NOT1 scaffold of the human CCR4-NOT deadenylase complex. *Nucleic Acids Res* **40**, 11058–11072.

10 Chen Y, Boland A, Kuzuoglu-Ozturk D, Bawankar P, Loh B, Chang CT, Weichenrieder O and Izaurralde E (2014) A DDX6-CNOT1 complex and W-binding pockets in CNOT9 reveal direct links between miRNA target recognition and silencing. *Mol Cell* **54**, 737–750.

11 Mathys H, Basquin J, Ozgur S, Czarnocki-Cieciura M, Bonneau F, Aartse A, Dziembowski A, Nowotny M, Conti E and Filipowicz W (2014) Structural and biochemical insights to the role of the CCR4-NOT complex and DDX6 ATPase in microRNA repression. *Mol Cell* **54**, 751–765.

12 Bhaskar V, Roudko V, Basquin J, Sharma K, Urlaub H, Seraphin B and Conti E (2013) Structure and RNA-binding properties of the Not1-Not2-Not5 module of the yeast Ccr4-Not complex. *Nat Struct Mol Biol* **20**, 1281–1288.

13 Boland A, Chen Y, Raisch T, Jonas S, Kuzuoglu-Ozturk D, Wohlbold L, Weichenrieder O and Izaurralde E (2013) Structure and assembly of the NOT module of the human CCR4-NOT complex. *Nat Struct Mol Biol* **20**, 1289–1297.

14 Pavanello L, Hall B, Airhihen B and Winkler GS (2018) The central region of CNOT1 and CNOT9 stimulate deadenylation by the Ccr4-Not nuclease module. *Biochem J* **475**, 3437–3450.

15 Stowell JAW, Webster MW, Kogel A, Wolf J, Shelley KL and Passmore LA (2016) Reconstitution of targeted deadenylation by the Ccr4-not complex and the YTH domain protein Mmi1. *Cell Rep* **17**, 1978–1989.

16 Chekulaeva M, Mathys H, Zipprich JT, Attig J, Colic M, Parker R and Filipowicz W (2011) miRNA repression involves GW182-mediated recruitment of CCR4-NOT through conserved W-containing motifs. *Nat Struct Mol Biol* **18**, 1218–1226.

17 Fabian MR, Cieplak MK, Frank F, Morita M, Green J, Srikumar T, Nagar B, Yamamoto T, Raught B, Duchaine TF *et al.* (2011) miRNA-mediated deadenylation is orchestrated by GW182 through two conserved motifs that interact with CCR4-NOT. *Nat Struct Mol Biol* **18**, 1211–1217.

18 Sandler H, Kreth J, Timmers HT and Stoecklin G (2011) Not1 mediates recruitment of the deadenylase Caf1 to mRNAs targeted for degradation by tristetraprolin. *Nucleic Acids Res* **39**, 4373–4386.

19 Bulbrook D, Brazier H, Mahajan P, Kliszczak M, Fedorov O, Marchese FP, Aubareda A, Chalk R, Picaud S, Strain-Damerell C *et al.* (2018) Tryptophan-mediated interactions between Tristetraprolin and the CNOT9 subunit are required for CCR4-NOT deadenylase complex recruitment. *J Mol Biol* **430**, 722–736.

20 Fabian MR, Frank F, Rouya C, Siddiqui N, Lai WS, Karetnikov A, Blackshear PJ, Nagar B and Sonenberg N (2013) Structural basis for the recruitment of the human CCR4-NOT deadenylase complex by tristetraprolin. *Nat Struct Mol Biol* **20**, 735–739.

21 Washio-Oikawa K, Nakamura T, Usui M, Yoneda M, Ezura Y, Ishikawa I, Nakashima K, Noda T, Yamamoto T and Noda M (2007) Cnot7-null mice exhibit high bone mass phenotype and modulation of BMP actions. *J Bone Miner Res* **22**, 1217–1223.

22 Berthet C, Morera AM, Asensio MJ, Chauvin MA, Morel AP, Dijoud F, Magaud JP, Durand P and Rouault JP (2004) CCR4-associated factor CAF1 is an essential factor for spermatogenesis. *Mol Cell Biol* **24**, 5808–5820.

23 Nakamura T, Yao R, Ogawa T, Suzuki T, Ito C, Tsunekawa N, Inoue K, Ajima R, Miyasaka T, Yoshida Y *et al.* (2004) Oligo-astheno-teratozoospermia in mice lacking Cnot7, a regulator of retinoid X receptor beta. *Nat Genet* **36**, 528–533.

24 Morita M, Oike Y, Nagashima T, Kadomatsu T, Tabata M, Suzuki T, Nakamura T, Yoshida N, Okada M and Yamamoto T (2011) Obesity resistance and increased hepatic expression of catabolism-related mRNAs in Cnot3(+/-) mice. *EMBO J* **30**, 4678–4691.

25 De Keersmaecker K, Atak ZK, Li N, Vicente C, Patchett S, Girardi T, Gianfelici V, Geerdens E, Clappier E, Porcu M *et al.* (2013) Exome sequencing identifies mutation in CNOT3 and ribosomal genes RPL5 and RPL10 in T-cell acute lymphoblastic leukemia. *Nat Genet* **45**, 186–190.

26 Wong SQ, Behren A, Mar VJ, Woods K, Li J, Martin C, Sheppard KE, Wolfe R, Kelly J, Cebon J, Dobrovic A *et al.* (2015) Whole exome sequencing identifies a recurrent RQCD1 P131L mutation in cutaneous melanoma. *Oncotarget* **6**, 1115–1127.

27 Faraji F, Hu Y, Wu G, Goldberger NE, Walker RC, Zhang J and Hunter KW (2014) An integrated systems genetics screen reveals the transcriptional structure of inherited predisposition to metastatic disease. *Genome Res* **24**, 227–240.

28 Faraji F, Hu Y, Yang HH, Lee MP, Winkler GS, Hafner M and Hunter KW (2016) Post-transcriptional control of tumor cell autonomous metastatic potential by CCR4-NOT deadenylase CNOT7. *PLoS Genet* **12**, e1005820.

29 Takahashi S, Kontani K, Araki Y and Katada T (2007) Caf1 regulates translocation of ribonucleotide reductase by releasing nucleoplasmic Spd1-Suc22 assembly. *Nucleic Acids Res* **35**, 1187–1197.

30 Temme C, Zhang L, Kremmer E, Ihling C, Chartier A, Sinz A, Simonelig M and Wahle E (2010) Subunits of the Drosophila CCR4-NOT complex and their roles in mRNA deadenylation. *RNA* **16**, 1356–1370.

31 Viswanathan P, Ohn T, Chiang YC, Chen J and Denis CL (2004) Mouse CAF1 can function as a processive deadenylase/3′-5′-exonuclease in vitro but in yeast the deadenylase function of CAF1 is not required for mRNA poly(A) removal. *J Biol Chem* **279**, 23988–23995.

32 Chen J, Chiang YC and Denis CL (2002) CCR4, a 3′-5′ poly(A) RNA and ssDNA exonuclease, is the catalytic component of the cytoplasmic deadenylase. *EMBO J* **21**, 1414–1426.

33 Niinuma S, Fukaya T and Tomari Y (2016) CCR4 and CAF1 deadenylases have an intrinsic activity to remove the post-poly(A) sequence. *RNA* **22**, 1550–1559.

34 Tucker M, Staples RR, Valencia-Sanchez MA, Muhlrad D and Parker R (2002) Ccr4p is the catalytic subunit of a Ccr4p/Pop2p/Notp mRNA deadenylase complex in Saccharomyces cerevisiae. *EMBO J* **21**, 1427–1436.

35 Maryati M, Airhihen B and Winkler GS (2015) The enzyme activities of Caf1 and Ccr4 are both required for deadenylation by the human Ccr4-Not nuclease module. *Biochem J* **469**, 169–176.

36 Webster MW, Chen YH, Stowell JAW, Alhusaini N, Sweet T, Graveley BR, Coller J and Passmore LA (2018) mRNA deadenylation is coupled to translation rates by the differential activities of Ccr4-not nucleases. *Mol Cell* **70** (1089–1100), e8.

37 Yi H, Park J, Ha M, Lim J, Chang H and Kim VN (2018) PABP cooperates with the CCR4-NOT complex to promote mRNA deadenylation and block precocious decay. *Mol Cell* **70** (1081–1088), e5.

38 Stupfler B, Birck C, Seraphin B and Mauxion F (2016) BTG2 bridges PABPC1 RNA-binding domains and CAF1 deadenylase to control cell proliferation. *Nat Commun* **7**, 10811.

39 Jadhav GP, Kaur I, Maryati M, Airhihen B, Fischer PM and Winkler GS (2015) Discovery, synthesis and biochemical profiling of purine-2,6-dione derivatives as inhibitors of the human poly(A)-selective ribonuclease Caf1. *Bioorg Med Chem Lett* **25**, 4219–4224.

40 Maryati M, Kaur I, Gopal J, Olotu-Umoren L, Oveh B, Hashmi L, Fischer PM and Winkler GS (2014) A fluorescence-based assay suitable for quantitative analysis of deadenylase enzyme activity. *Nucleic Acids Res* **42**, e30.

41 Mondal S, Hsiao K and Goueli SA (2016) A bioluminescent assay for monitoring conjugation of ubiquitin and ubiquitin-like proteins. *Anal Biochem* **510**, 41–51.

42 Mondal S, Hsiao K and Goueli SA (2017) Utility of adenosine monophosphate detection system for monitoring the activities of diverse enzyme reactions. *Assay Drug Dev Technol* **15**, 330–341.

43 Goueli SA, Hsiao K and Zegzouti H (2013) U.S. Patent. 2013/0109037 A1

44 Niesen FH, Berglund H and Vedadi M (2007) The use of differential scanning fluorimetry to detect ligand interactions that promote protein stability. *Nat Protoc* **2**, 2212–2221.

45 Klumpp K, Hang JQ, Rajendran S, Yang Y, Derosier A, Wong Kai In P, Overton H, Parkes KE, Cammack N and Martin JA (2003) Two-metal ion mechanism of RNA cleavage by HIV RNase H and mechanism-based design of selective HIV RNase H inhibitors. *Nucleic Acids Res* **31**, 6852–6859.

46 Parkes KE, Ermert P, Fässler J, Ives J, Martin JA, Merrett JH, Obrecht D, Williams G and Klumpp K (2003) Use of a pharmacophore model to discover a new class of influenza endonuclease inhibitors. *J Med Chem* **46**, 1153–1164.

47 Tumey LN, Bom D, Huck B, Gleason E, Wang J, Silver D, Brunden K, Boozer S, Rundlett S, Sherf B *et al.* (2005) The identification and optimization of a N-hydroxy urea series of flap endonuclease 1 inhibitors. *Bioorg Med Chem Lett* **15**, 277–281.

48 Exell JC, Thompson MJ, Finger LD, Shaw SJ, Debreczeni J, Ward TA, McWhirter C, Siöberg CL, Martinez Molina D, Abbott WM *et al.* (2016) Cellularly active N-hydroxyurea FEN1 inhibitors block substrate entry to the active site. *Nat Chem Biol* **12**, 815–821.

49 Lo MC, Aulabaugh A, Jin G, Cowling R, Bard J, Malamas M and Ellestad G (2004) Evaluation of fluorescence-based thermal shift assays for hit identification in drug discovery. *Anal Biochem* **332**, 153–159.

50 Pantoliano MW, Petrella EC, Kwasnoski JD, Lobanov VS, Myslik J, Graf E, Carver T, Asel E, Springer BA, Lane P *et al.* (2001) High-density miniaturized thermal shift assays as a general strategy for drug discovery. *J Biomol Screen* **6**, 429–440.